Indian Journal of Chemistry
Vol. 57A, March 2018, pp. 449-453

Sonochemical synthesis of ZnO, NiO and α-Fe_2O_3 nanoparticles and their catalytic activity for thermal decomposition of ammonium perchlorate

Seyed Ghorban Hosseini* & Zahra Khodadadipoor

Department of Chemistry, Malek Ashtar University of Technology, P.O. Box 16765-3454, Tehran, Iran

Email: hoseinitol@yahoo.com

ZnO, NiO and α-Fe_2O_3 nanoparticles are synthesized by a simple and facile sonochemical calcination of zinc acetate, nickel acetate, and iron chloride as precursors. The as-prepared products are characterized by powder X-ray diffraction, and field emission scanning electron microscopy. The catalytic efficiency of these as-prepared oxides for thermal decomposition of ammonium perchlorate has been investigated by thermal gravimetric analysis and differential scanning calorimetry. The results show that addition of 2% as-prepared samples leads to merging of the two exothermic peaks of ammonium perchlorate into one peak. In the presence of ZnO and NiO nanoparticles, the high temperature decomposition peak of ammonium perchlorate decreases by about 120 °C and 105 °C, respectively. In the presence of α-Fe_2O_3 nanoparticles, the high temperature decomposition peak of ammonium perchlorate decreases by 67 °C, while the peak of the low temperature decomposition disappears.

Keywords: Thermal decomposition, Ammonium perchlorate, Oxides, Metal oxides, Nanoparticles, Sonochemical synthesis

Ammonium perchlorate (AP) is one of the most common oxidizing agents used in composite solid propellants (CSP). Thermal decomposition of AP has a major role on the performance of CSPs. Decrease in the high-temperature decomposition (HTD) and increase in the specific heat release of AP are important factors for enhancing the burning rate of CSPs[1-3]. The application of superfine AP can enhance the performance of propellants, but the preparation of superfine AP is hazardous. Therefore, many researchers have investigated different catalysts for thermal decomposition of AP to improve the combustion behavior of solid propellant[5-7].

In the last few decades, many transition metal oxides (TMOs) including CoO, CuO, Co_3O_4, Fe_2O_3 etc., have been studied for the thermal decomposition of AP[8-10]. Since the catalytic activity of metal oxides is significantly related to their surface area, metal oxide nanoparticles have attracted greater attention than bulk metal oxides for thermal decomposition of AP[11, 12]. Among these, ZnO as an n-type semiconductor with a wide direct band gap (3.37 eV) has attracted wide interest due to its low cost, non-toxicity, and good electrical property. Various methods such as sol-gel, soft chemical method, vapor phase growth, etc., have been reported for the synthesis of ZnO nanoparticles[13-15]. For the synthesis of nanocrystalline NiO (an important p-type semiconductor widely used in catalysis) from different precursor materials, several methods such as thermal decomposition, precipitation and solvothermal method have been reported[16-19]. The catalytic activity of hematite nanoparticles (α-Fe_2O_3 NPs) in the thermal decomposition of AP has also been reported[20-22]. Several chemical methods, such as solvothermal, laser pyrolysis, thermal oxidation and hydrothermal method, have been reported for synthesis of α-Fe_2O_3 NPs[23-25]. However, these synthesis methods have many disadvantages, including use of expensive, toxic and potentially hazardous chemicals, high production cost, and low production. Several studies on decomposition of AP using ZnO, NiO and α-Fe_2O_3 have reported excellent catalytic activities[12, 20, 26, 27]. The porous ZnO nanospheres prepared by Yang *et al*.[28] decreased the decomposition temperature of AP by 130 °C. Sun *et al*.[29] reported that in the presence of ZnO twin-cones the thermal decomposition temperature of AP was reduced by 120 °C. NiO nanorods prepared by hydrothermal method decreased the thermal decomposition temperature of AP by 65 °C[30]. We have reported earlier that in the presence of spherical α-Fe_2O_3 NPs prepared by high energy ball-milling method, the thermal decomposition temperature of AP decreased by ~61 °C[31].

Compared to other methods, the sonochemical method is simple, very fast, does not need high temperatures and surfactants and yields crystalline phase as-prepared samples[32]. The effects of ultrasound radiation on chemical reactions are due to the very high temperatures and pressures that develop during the sonochemical cavity collapse by acoustic cavitation. To the best of our knowledge, there is no

report on the use of ZnO, NiO and α-Fe_2O_3 NPs synthesized by ultrasonic method as catalysts on the thermal decomposition, heat of decomposition and kinetic parameters of AP particles. In the present work, ZnO, NiO and and α-Fe_2O_3 NPs were prepared by a facile ultrasonic method. Then nanocomposites of AP and as-prepared nanoparticles were prepared by the solvent/non-solvent method, as a conventional microencapsulation technique. The catalytic effect of the as-prepared ZnO, NiO and α-Fe_2O_3 NPs on the thermal decomposition of AP was investigated by thermogravimetric analysis (TGA) and differential scanning calorimetry (DSC).

Experimental

All chemicals including $Zn(CH_3COO)_2.2H_2O$, $Ni(CH_3COO)_2$, $FeCl_3.6H_2O$, NaOH, ethanol, and toluene were purchased from Merck. AR grade NH_4ClO_4 powder with a mean particle size of 80–100 μm was obtained from Fluka. Doubly distilled water was used in these experiments. X-ray powder diffraction data were collected using a Bruker D8 Advance powder diffractometer using Cu-Kα radiation over a 2θ range of 10–90° with a 0.05° step size. The crystallite sizes of the as-prepared samples were estimated by the Scherrer method. Field emission scanning electron microscope (FESEM) analysis (Zeiss Sigma) was used to investigate the morphology, particle size and agglomeration of the powders. Investigation of thermal behavior of nanocomposites was carried out using a TGA/DSC simultaneous thermal analyzer (Mettler Toledo) at a heating rate of 10 °C min^{-1} in air. A multiwave ultrasonic generator (Sonicator-3000; Misonix, Inc., Farmingdale, NY, USA), equipped with a converter/transducer and titanium oscillator (horn) (10 mm in dia.) operating at 45 kHz with a maximum power output of 600 W, was used for the ultrasonic irradiation. The ultrasonic generator could automatically adjust the required power level. The ZnO, NiO and α-Fe_2O_3 NPs were dispersed in the non-solvent by an ultrasonic (LAB Sonic RP) apparatus.

To prepare the NiO and ZnO NPs, NaOH (100 mL, 0.1 M) was added to 50 mL of 0.1 M ethanolic solutions of $Ni(CH_3COO)_2$ and $Zn(CH_3COO)_2.2H_2O$, respectively. Then the suspension was ultrasonically irradiated with a high-density ultrasonic probe immersed directly into the solution. The mixtures were sonicated at 60 W ultrasound power for 35 min.

To synthesize α-Fe_2O_3 nanoparticles, NaOH (50 mL, 0.3 M) was added dropwise to $FeCl_3.6H_2O$ solution (0.1 M) over a period of 30 min. The obtained yellow slurry was sonicated with 60 W ultrasound power for 45 min. Finally, the ZnO (milky precipitate), NiO (green precipitate) and Fe_2O_3 (red brown precipitate) were separated by vacuum filtering and then washed three times with methanol and doubly distilled water to remove impurities. The ZnO sample was heated in a furnace at 400 °C for 4 h to obtain the white ZnO powder. Crystalline NiO and Fe_2O_3 nanoparticles were obtained on heating the respective samples at 500 °C for 2 h and 1 h respectively.

The AP/ZnO, AP/NiO and AP/α-Fe_2O_3 nanocomposites (2% by mass of nanoparticles) were prepared by solvent/non-solvent method[13]. In this experiment, water and toluene were chosen as the solvent and non-solvent respectively. Typically, 200 mg of the synthesized nanoparticles (ZnO or α-Fe_2O_3 or NiO) was dispersed in 15 mL toluene ultrasonically for 20 min (solution A). Then, 0.98 g AP was dissolved in 8 mL water to make a saturated solution at 80 °C. The saturated solution of AP was added dropwise to solution A, to obtain the nanocomposite. In the reaction lasting several minutes, all the AP particles were deposited on the surface of metal oxide nanoparticles. Finally, the coated particles (i.e., composites) were filtered, washed and dried at ambient temperature.

Results and discussion

The reaction between nickel acetate or zinc acetate or iron chloride and NaOH to form nickel oxide or zinc oxide or iron oxide (hematite) is shown in Scheme 1. The XRD patterns of NiO, ZnO and α-Fe_2O_3 NPs show that the crystalline phases of NiO and ZnO are cubic (JCPD 78-0643) and hexagonal (JCPDS 36-1451 space group $P6_3mc$, with lattice

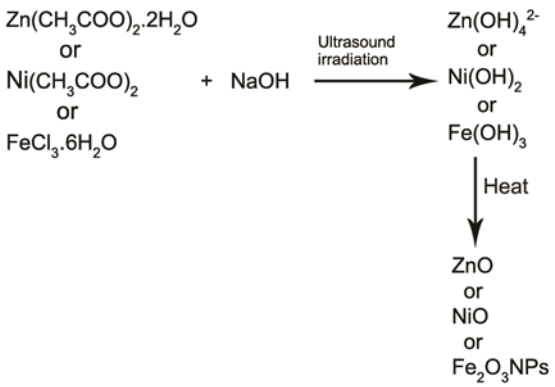

Mechanism of NiO, ZnO and α-Fe2O3 NPs formation

Scheme 1

constants, a = 3.24982 Å, c = 1.6021 Å, Z = 2), respectively (Fig. 1(curves 1 & 2)). As can be seen from Fig. 1(curve 3) almost all the diffraction peaks can be well assigned to α-Fe_2O_3, with a rhombohedral phase (R3c, JCPDS 01-1053, a = 0.5028 nm, c = 1. 3730 nm). Absence of any other characteristic peak, indicated that the products are of high purity. Broadening of the peaks indicated that the particles were of nanometer scale. From the Scherrer formula, $D = 0.891\ \lambda/\beta \cos\theta$, the average size of the ZnO nanoparticles after calcination at 400°C for 4 h was calculated to be ~57.5 nm. For NiO after heating at 500 °C for 2 h, the average particle size was ~70 nm and for Fe_2O_3 after heat treatment at 500°C for 1 h, it was ~20 nm, which is in agreement with the SEM images.

Since the catalytic activity of metal oxides nanoparticles depend on their morphology and size. the structure, morphology and size of the samples were investigated by field scanning electron microscopy (FESEM). The morphology of the ZnO and NiO nanoparticles is approximately spherical with the diameter varying between 40 and 80 nm (Fig. 2(a&b). Formation of spherical grains with good uniform distribution is observed in the case of α-Fe_2O_3 NPs. In the present study, the morphology of the as-prepared nanoparticles remained spherical with a high degree of crystallinity. The ultrasonic assisted method can be easily controlled and may find application in the preparation of other nanoparticles.

The effect of NiO, ZnO and α-Fe_2O_3 NPs on the thermal behavior of ammonium perchlorate was studied by thermogravimetry (TG) and differential scanning calorimetry (DSC). Figure 3 shows the DSC curves for pure AP as well as AP/ZnO, AP/NiO, AP/α-Fe_2O_3 nanocomposites at a heating rate of 10 °C min^{-1} under air atmosphere. It was observed that for pure AP, the first endothermic peak is

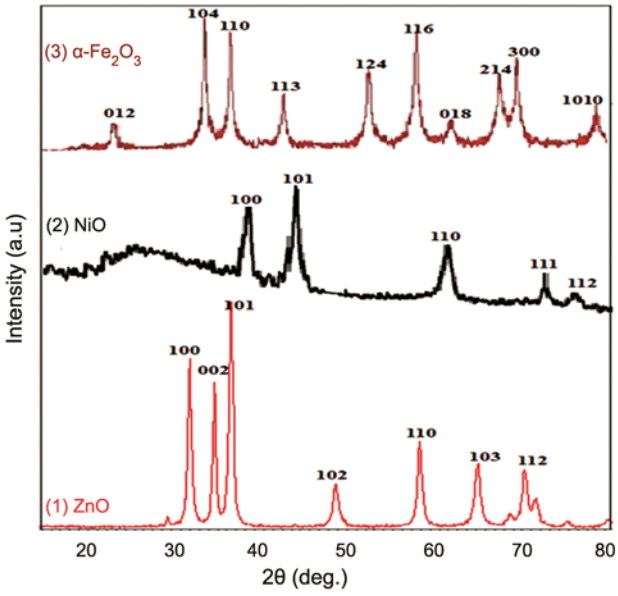

Fig. 1 – XRD patterns of ZnO (1), NiO (2) and α-Fe_2O_3 NPs (3).

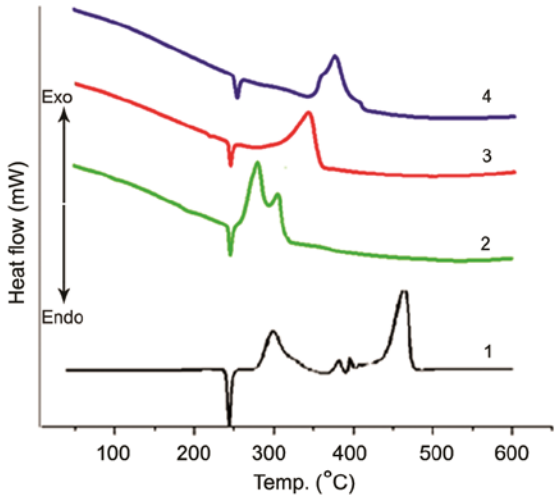

Fig. 3 – DSC curves for pure AP (1) and AP/ZnO (2), AP/NiO (3) and AP/α-Fe_2O_3 (4) nanocomposites. [heating rate: 10 °C min^{-1}].

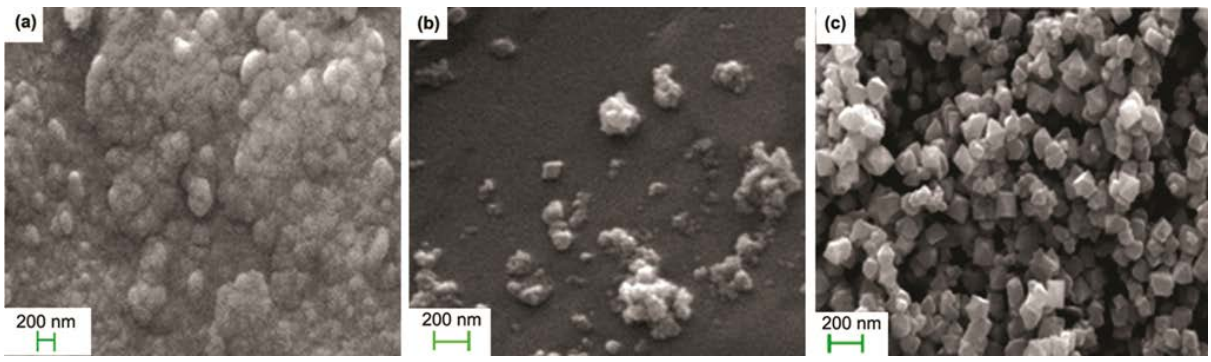

Fig. 2 – FESEM images of (a) ZnO, (b) NiO, and (c) α-Fe2O3 nanoparticles.

centered at 240 °C, indicating crystal transformation of AP from orthorhombic to cubic phase. The second exothermic peak (LTD) at 310 °C shows the partial decomposition of AP, while the third exothermic peak (HTD) at ~432 °C corresponds to the complete decomposition of AP[33, 34]. When ZnO, NiO or α-Fe_2O_3 NPs were added, the first endothermic peak appeared at the same position as that of pure AP, showing that the catalysts have no influence on the crystallographic transition temperature. However, in the presence of ZnO, NiO or α-Fe_2O_3 NPs, the high temperature decomposition peak decreased and merged into one exothermic peak at 312, 327 and 365 °C, respectively. Furthermore, the total heat release (Δ*H*) of thermal decomposition of AP increased from 590 J g^{-1} to 1215 J g^{-1} in the case of AP/ZnO and to 1224 J g^{-1} with AP/NiO. Table 1 shows that these nanoparticles can effectively decrease the first and second decomposition temperatures and increase the enthalpy of decomposition of AP.

The TGA curves of pure AP and mixture of AP with the as-prepared catalysts are shown in Fig. 4. From room temperature to 600 °C, two weight loss steps are observed for pure AP, whereas for AP/ZnO, AP/NiO and AP/α-Fe_2O_3 nanocomposites, only one weight loss step is observed. This is in good agreement with the DSC results. The thermal decomposition process of AP is a complex hetero-phase process including coupled reactions in the solid, absorbed and gaseous phases[35]. Many studies have shown that thermal decomposition of AP proceeds through electron transfer from perchlorate ion to ammonium ion. According to the electron transfer theory, ammonia oxidation and dissociation of ClO_4^- species into ClO_3^- and O_2 are the two important steps for AP decomposition. Metal oxides exhibit high catalytic activity towards ammonia oxidation and enhance the dissociation of ClO_4^- species into ClO_3^- and O_2[36]. Proton transfer theory is another mechanism proposed for thermal decomposition of AP. Since AP is a typical dielectric, thermal decomposition of AP at low temperature cannot proceed through electron transfer[37]. There are three steps in the proton transfer mechanism; Step I includes a pair of ions in the AP lattice. Decomposition of AP occurs in Step II through proton transfer from NH_4^+ to ClO_4^-. Then ammonia and perchloric acid are formed from decomposition of the molecular complex in Step III, as follows:

$$NH_4ClO_4 \leftrightarrow NH_3 - H - ClO_4^- \leftrightarrow NH_3(a) + HClO_4(a) \leftrightarrow NH_3(g) + HClO_4(g)$$

Many reactions occur between NH_3 and $HClO_4$ in the gas phase to form side products such as O_2, N_2O, Cl_2, NO, and H_2O at low temperatures (LTD). Generally, during low temperature thermal decomposition, the reaction between $HClO_4$ and NH_3 is incomplete and the residual NH_3 is adsorbed on the surface of the AP particles, leading to saturation of ammonia[38]. As a result, the rate of high temperature decomposition decreases. Since nanoparticles have a larger surface area in comparison with bulk particles, there are many more active sites on their surface. These nanoparticles adsorb the gaseous ammonia molecules on their surface to catalyze the reaction and thus, decrease the high temperature decomposition of AP.

Catalytic activity of ZnO, NiO and α-Fe_2O_3 synthesized by other methods have been investigated for the high-temperature decomposition (HTD) of AP particles[28, 39]. The catalytic activities of ZnO, NiO and α-Fe_2O_3 NPs synthesized by ultrasonic method herein are comparable with the chemically synthesized ZnO, NiO and α-Fe_2O_3 NPs reported earlier[12, 39-41] (Supplementary data, Table S1).

Table 1 – Thermal decomposition of AP in the presence of 2% and 4% ultrasonically synthesized ZnO, NiO and α-Fe_2O_3 nanoparticles

Samples	Avg particle size (nm)	LTD (°C)	HTD (°C)	ΔH (J g^{-1})
Pure AP		297	432	590
AP + 2% ZnO	57.7	-	312	1215.42
AP + 2% NiO	70	-	327	1224.33
AP + 2% α-Fe_2O_3	20	-	365	1325.12

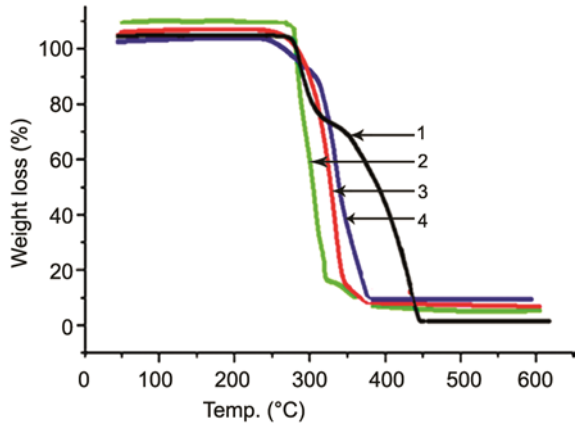

Fig. 4 – TGA curves for pure AP (1) and AP/ZnO (2), AP/NiO (3) and AP/α-Fe_2O_3 (4) nanocomposites.

In this work, we have synthesized NiO, ZnO and α-Fe_2O_3 NPs via a simple sonochemical method. The as-prepared nanoparticles were characterized by XRD, and FESEM. The average particle sizes of NiO, ZnO and α-Fe_2O_3 NPs were estimated to be ~70, 57.7 and 20 nm, respectively. The catalytic activities of the as-prepared metal oxides for thermal decomposition of AP were studied by TGA/ DSC technique. The TGA-DSC results showed that these NPs have good catalytic properties for the thermal decomposition of AP; the exothermic heat release increased 2.5 folds in comparison with that of the pure AP.

Supplementary data

Supplementary data associated with this article are available in the electronic form at http://www.niscair.res.in/jinfo/ijca/IJCA_57A(03)449-453_SupplData.pdf.

References

1 Liu Z T, Li X, Liu Z W & Lu J, *Powder Technol*, 189 (2009) 514.
2 Duan G, Yang X, Chen J, Huang G, Lu L & Wang X, *Powder Technol*, 172 (2007) 27.
3 Hosseini S G, Ahmadi R, Ghavi A & Kashi A, *Powder Technol*, 278 (2015) 316.
4 Chen L, Li L & Li G, *J Alloys Compd*, 464 (2008) 532.
5 Chen L & Zhu D, *Solid State Sci*, 27 (2014) 69.
6 Chaturvedi S & Dave P N, *J Exp Nanosci*, 7 (2012) 205.
7 Alizadeh-Gheshlaghi E, Shaabani B, Khodayari A, Azizian-Kalandaragh Y & Rahimi R, *Powder Technol*, 217 (2012) 330.
8 Ayoman E & Hosseini S G, *J Therm Anal Calorim*, 123 (2016) 1213.
9 Hosseini S G, Toloti S J H, Babaei K & Ghavi A, *J Therm Anal Calorim*, 124 (2016) 1243.
10 Joshi S S, Patil P R & Krishnamurthy V, *Def Sci J*, 58 (2008) 721.
11 Lucas E, Decker S, Khaleel A, Seitz A, Fultz S, Ponce A, Li W, Carnes C & Klabunde K J, *Chem Eur J*, 7 (2001) 2505.
12 Wang Y, Zhu J, Yang X, Lu L & Wang X, *Thermochim Acta*, 437 (2005) 106.
13 Vafaee M & Ghamsari M S, *Mater Lett*, 61 (2007) 3265.
14 Wu C, Qiao X, Chen J, Wang H, Tan F & Li S, *Mater Lett*, 60 (2006) 1828.
15 Sun X, Zhang H, Xu J, Zhao Q, Wang R & Yu D, *Solid State Commun*, 129 (2004) 803.
16 Song X, Gao L & Mathur S, *J Phys Chem C*, 115 (2011) 21730.
17 El-Kemary M, Nagy N & El-Mehasseb I, *Mater Sci Semicond Process*, 16 (2013) 1747.
18 Imran Din M & Rani A, *Int J Anal Chem*, 2016 (2016) 1.
19 Zhu Z, Wei N, Liu H & He Z, *Adv Powder Technol*, 22 (2011) 422.
20 Ma Z Y, Li F S, Chen A S & Bai H P, *Acta Chim Sin*, 62 (2004) 1252.
21 Ma Z, Wu R, Song J, Li C, Chen R & Zhang L, *Propel Explos Pyrotech*, 37 (2012) 183.
22 Song L, Zhang S, Chen B, Ge J & Jia X, *Colloids Surf A: Physicochem Eng Asp*, 360 (2010) 1.
23 Zhu D, Zhang J, Song J, Wang H, Yu Z, Shen Y & Xie A, *Appl Surf Sci*, 284 (2013) 855.
24 Dumitrache F, Morjan I, Fleaca C, Badoi A, Manda G, Pop S, Marta D, Huminic G, Huminic A & Vekas L, *Appl Surf Sci*, 336 (2015) 297.
25 Su X, Yu C & Qiang C, *Appl Surf Sci*, 257 (2011) 9014.
26 Solymosi F & Revesz L, *Nature*, 192 (1961) 64.
27 Zhang Y, Liu X, Nie J, Yu L, Zhong Y & Huang C, *J Solid State Chem*, 184 (2011) 387.
28 Yang J M, Zhang W, Liu Q & Sun W Y, *RSC Adv*, 4 (2014) 51098.
29 Sun X, Qiu X, Li L & Li G, *Inorg Chem*, 47 (2008) 4146.
30 Zhao Y, Zhang X, Xu X, Zhao Y, Zhou H, Li J & Jin H, *CrystEngComm*, 18 (2016) 4836.
31 Hosseini S G & Ayoman E, *J Thermal Anal Calorim*, 128 (2017) 915.
32 Bang J H & Suslick K S, *Adv Mater*, 22 (2010) 1039.
33 Zhang Y, Liu X, Chen D, Yu L, Nie J, Yi S, Li H & Huang C, *J Alloys Compd*, 509 (2011) L69.
34 Reid D L, Russo A E, Carro R V, Stephens M A, LePage A R, Spalding T C, Petersen E L & Seal S, *Nano Lett*, 7 (2007) 2157.
35 Jia Z, Ren D, Wang Q & Zhu R, *Appl Surf Sci*, 270 (2013) 312.
36 Zhang Y & Meng C, *J Alloys Compd*, 674 (2016) 259.
37 Boldyrev V, *Thermochim Acta*, 443 (2006) 1.
38 Hosseini S G, Abazari R & Gavi A, *Solid State Sci*, 37 (2014) 72.
39 Wang J G, Jin L N, Qian X Y & Dong M D, *J Nanosci Nanotechnol*, 16 (2016) 8635.
40 Hosseini S G & Ayoman E, *Indian J Chem*, 56A (2017) 592.
41 Babar Z U D & Malik A Q, *Combust Sci Technol*, 187 (2015) 1295.